

ZnO homojunction photodiodes based on Sb-doped p-type nanowire array and n-type film for ultraviolet detection

Guoping Wang,¹ Sheng Chu,¹ Ning Zhan,¹ Yuqing Lin,² Leonid Chernyak,² and Jianlin Liu^{1,a)}

¹*Department of Electrical Engineering, Quantum Structures Laboratory, University of California at Riverside, Riverside, California 92521, USA*

²*Department of Physics, University of Central Florida, Orlando, Florida 32816-2385, USA*

(Received 23 November 2010; accepted 13 January 2011; published online 28 January 2011)

ZnO p-n homojunctions based on Sb-doped p-type nanowire array and n-type film were grown by combining chemical vapor deposition (for nanowires) with molecular-beam epitaxy (for film). Indium tin oxide and Ti/Au were used as contacts to the ZnO nanowires and film, respectively. Characteristics of field-effect transistors using ZnO nanowires as channels indicate p-type conductivity of the nanowires. Electron beam induced current profiling confirmed the existence of ZnO p-n homojunction. Rectifying I-V characteristic showed a turn-on voltage of around 3 V. Very good response to ultraviolet light illumination was observed from photocurrent measurements. © 2011 American Institute of Physics. [doi:10.1063/1.3551628]

ZnO has a wide band gap of 3.37 eV and a large exciton binding energy of 60 meV at room temperature,^{1,2} which make it a promising candidate for optoelectronic devices such as blue-light emitting diodes,^{3,4} ultraviolet (UV) laser diodes,⁵⁻⁷ and photodiodes.⁸⁻¹⁰ Recently, there have been tremendous interests in ZnO nanowire arrays. Although heterojunction optoelectronic devices¹¹⁻¹³ have been fabricated based on vertically aligned ZnO nanowire arrays, there still lacks the homojunction type devices based on p-type nanowire array/n-type ZnO film. It is well known that one of the biggest challenges toward good ZnO-based optoelectronic devices is the difficulty of reliably fabricating p-type ZnO due to the self-compensating effect from native defects (for example, oxygen vacancy V_o and zinc interstitial Zn_i) and/or H incorporation.¹⁴ Nevertheless, there has already been a great deal of efforts on the fabrication of p-type ZnO by doping group V elements, such as N, P, and As.¹⁵⁻¹⁷ Previously, our group showed that Sb, another group V element, is an effective dopant for reproducible p-type ZnO thin films¹⁸ on Si and sapphire substrates. Heterojunction⁸ and homojunction⁹ light emitting diodes as well as photodiodes based on these films were achieved. In this study, we report ZnO p-n homojunctions based on Sb-doped p-type ZnO nanowire arrays grown by chemical vapor deposition (CVD) on n-type ZnO films on sapphire substrates grown by molecular-beam epitaxy (MBE). The homojunction diode exhibits a clear rectification characteristic as well as very good ultraviolet light absorption characteristics.

The device fabrication process of the p-type ZnO nanowire/n-type ZnO film structure is described as follows. A highly oriented vertical ZnO nanowire array was synthesized via seed growth method.¹⁹ First, n-type ZnO seed film, which also acted as n-type component of the junction, was grown on a 2 in. c-plane sapphire substrate using plasma-assisted MBE. The growth process began with a thin MgO/ZnO buffer layer of less than 10 nm at a growth temperature of 550 °C for improving the subsequent ZnO film quality. Then the seed ZnO film was grown at 700 °C for 5 h, yield-

ing a total thickness of around 1050 nm. Elemental Zn was evaporated at an effusion cell temperature of 360 °C. The oxygen plasma was generated using a radio-frequency plasma source. The oxygen flow rate was kept at 5 sccm. Hall effect measurements were carried out on the MBE-grown ZnO thin film. The film was found to have n-type conductivity with an electron concentration of $3.74 \times 10^{17} \text{ cm}^{-3}$, a mobility of $23.04 \text{ cm}^2 \text{ V}^{-1} \text{ s}^{-1}$, and a resistivity of $0.73 \text{ } \Omega \text{ cm}$, respectively. The ZnO seed film was partially covered for exposing the film for later n-type contact deposition and then subsequently transferred into a quartz tube furnace system. The growth of nanowire array was carried out at 650 °C for 15 min with a gas flow of 1000 sccm nitrogen and 200 sccm mixture gas of argon/oxygen (99.5:0.5). A Zn powder source (99.999%) in a glass bottle was placed in the center of the quartz tube. At the place of $\sim 5 \text{ cm}$ upstream to the Zn powder source, Sb powder (99.99%) was placed in an open glass boat. The ZnO seed film was kept around 10 cm away from the Zn source on the downstream side. After a vertical nanowire array was achieved in CVD, polymethyl-methacrylate (PMMA) was spun on the sample to separate the bottom ZnO film and the subsequent top indium tin oxide (ITO) contact layer. The spin speed was 2000 rpm for 30 s, and this process was repeated for five times. After the sample was dried, a thin layer of ITO was sputtered by a sputter evaporator on the top of ZnO nanowire array. The sputtering process was performed at room temperature and the pressure was maintained at 10^{-2} Torr . The sputtering power and time were 180 W and 10 min, respectively. After the growth of ITO, acetone was used to remove the PMMA layer. The device was finished by depositing Ti/Au (20 nm/100 nm) on the n-type ZnO film using an electron-beam (e-beam) evaporator and rapidly annealed under 600 °C for 1 min to improve conductivity. Another low-resistant ITO glass slide was placed on the top of the ZnO nanowire array when I-V and photoresponse characteristics were measured. Figure 1 shows a schematic diagram of the device.

Figures 2(a) and 2(b) show scanning electron microscopy (SEM) images of the nanowire array from the top and

^{a)}Electronic mail: jianlin@ee.ucr.edu.

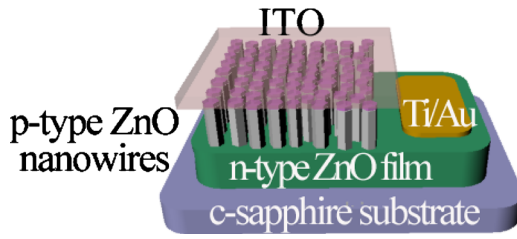


FIG. 1. (Color online) Schematic view of the photodetector device, which consists of ZnO thin film on c-sapphire substrate, vertically aligned ZnO nanowires, ITO contacts, and Ti/Au contacts.

the side, respectively. Typical wurtzite hexagonal structure ZnO nanowires are evident. The length and diameter of the ZnO nanowires are on average $3 \mu\text{m}$ and 150 nm , respectively. The single-crystalline nature of the ZnO nanowires is confirmed by high-resolution transmission electron microscopy (TEM) analysis, as shown in Fig. 2(c) and by the selected area electron diffraction (SAED) pattern [Fig. 2(d)].

Figure 3(a) shows spectrum of the electron beam induced current (EBIC) profiling of the homojunction between the ZnO nanowires and ZnO film superimposed on the side-view SEM image of the device. As a versatile tool, EBIC was widely used to identify buried junctions in semiconductors, including characterization of ZnO thin film p-n junctions²⁰ and silicon nanowire p-n junctions.²¹ In the experiment, electron-hole pairs are generated by electron beam irradiation. Then they are separated by built-in electric field in the p-n junction depletion region and collected by an external amplifier. Here, an accelerating voltage of 30 kV was applied, corresponding to the electron penetration depth of $1.5 \mu\text{m}$. Silver paste instead of ITO glass was used as contact to the p-type nanowires for facilitating the EBIC experiment. As seen from Fig. 3(a), an EBIC signal forms a peak on the thin film/nanowire junction, indicating the formation of p-n junction. The second peak on the right is due to the formation of the nanowire/ITO/silver paste semiconductor-metal junction.

The p-type conductivity of the Sb-doped ZnO nanowires can also be proved by field-effect measurement. ZnO nanowire field-effect transistors (NWFETs) were fabricated by standard photolithography. Sb-doped ZnO nanowires were transferred to a p⁺-silicon wafer with a 300 nm thick silicon oxide on the surface. Microcontact windows were defined on the ends of the nanowires, then Ni/Au ($20 \text{ nm}/100 \text{ nm}$) elec-

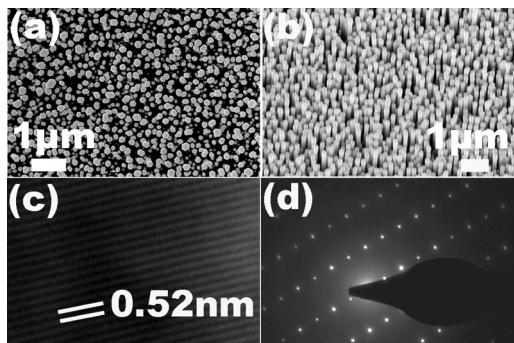


FIG. 2. (a) Top-view and (b) side-view SEM images of as-grown p-type ZnO nanowires. (c) High-resolution TEM image of a single nanowire. The lattice spacing between two atomic layers is measured to be 0.52 nm . (d) SAED pattern, indicating the single-crystalline characteristic of the nanowire.

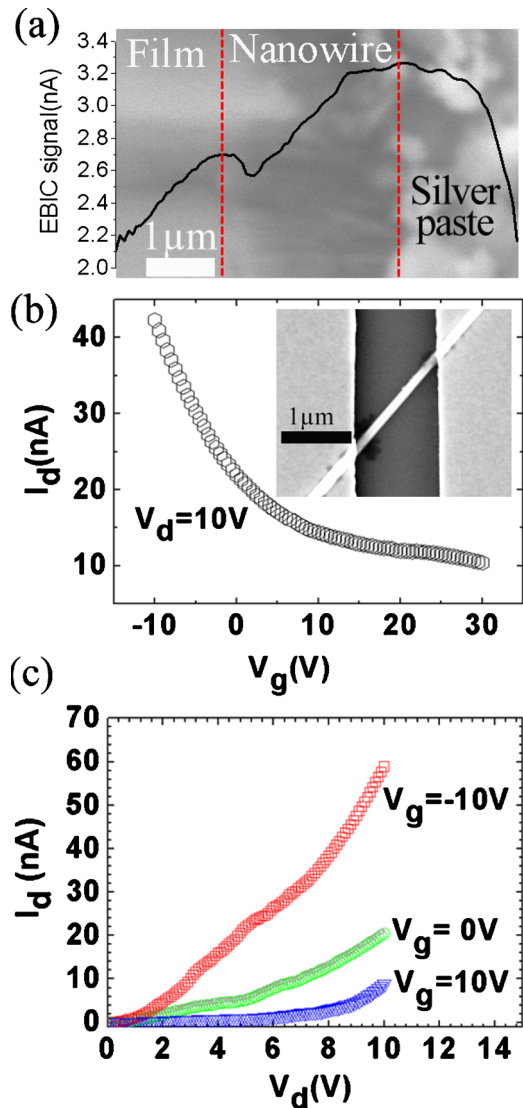


FIG. 3. (Color online) (a) EBIC profile of the device. A clear peak can be seen in the area between the ZnO nanowires and ZnO film, representing the formation of junction. (b) I_d - V_g curve of the ZnO nanowire FET under $V_d = 10 \text{ V}$. Inset shows the SEM image of the NWFET. (c) I_d - V_d curves of the ZnO nanowire FET recorded at different gate voltages.

trodes were formed by e-beam deposition and subsequent lift-off. The p⁺-silicon substrate served as the backgate electrode of the transistor. The inset in Fig. 3(b) shows the SEM image of the NWFET. The drain current (I_d) versus gate voltage (V_g) curve under a drain voltage (V_d) of 10 V and I_d versus V_d curves under different gate voltages are shown in Figs. 3(b) and 3(c), respectively. The results show that the Sb-doped ZnO nanowires exhibit p-type behavior under gate voltage ranging from -10 to 30 V . The origination of the p-type conductivity of the Sb-doped ZnO nanowires is from the shallow acceptors formed by substitutional Sb_{Zn} simultaneously connecting two Zn vacancies.²² The hole concentration (P) in nanowires can be estimated by using the following equation:²³

$$P = \left(\frac{V_{\text{th}}}{q} \right) \left[\frac{2\pi\epsilon_r\epsilon_0}{\ln(4h/d)} \right] \left(\frac{1}{\pi d^2/4} \right), \quad (1)$$

where ϵ_r , ϵ_0 , h , d , V_{th} , and q are the effective dielectric constant (3.9 for SiO_2), the dielectric constant in vacuum, the thickness of dielectric layer (300 nm), the nanowire diameter

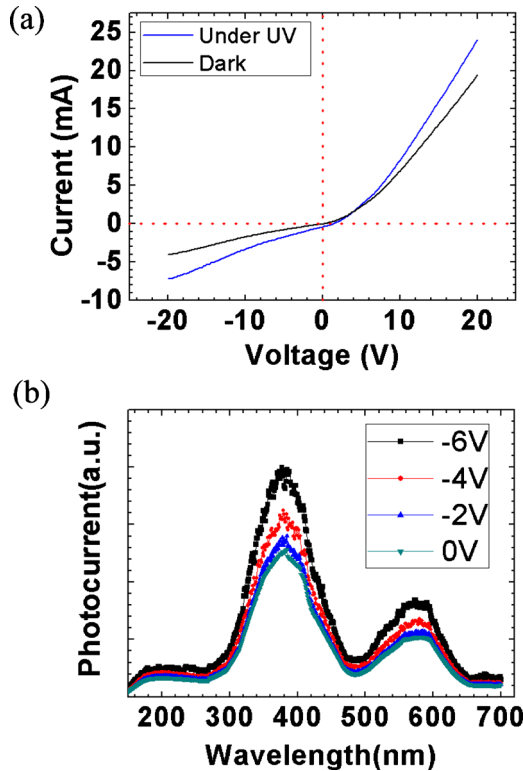


FIG. 4. (Color online) (a) I-V characteristics of the ZnO nanowire/ZnO film device with and without UV illumination. (b) PC spectra under different reverse biases. Good responses in the UV region are evident.

(~ 200 nm), the threshold voltage of the ZnO NWFET (~ 29 V), and the elementary charge constant, respectively. From Eq. (1), the hole concentration is calculated to be $6.9 \times 10^{17} \text{ cm}^{-3}$. The mobility can be calculated by using the equation²³

$$\mu = \left(\frac{dI}{dV_g} \right) \left[\frac{\ln\left(\frac{4h}{d}\right)}{2\pi\epsilon_r\epsilon_0} \right] \left(\frac{L}{V_d} \right), \quad (2)$$

where μ , L , and V_d are the mobility, the channel length ($\sim 1.8 \mu\text{m}$), and the drain-source voltage (10 V), respectively. $dI/dV_g = 2.55e-009 \text{ A/V}$ can be extrapolated from the linear region of the I_d-V_g curve. From Eq. (2), the mobility is calculated as approximately $0.037 \text{ cm}^2 \text{ V}^{-1} \text{ s}^{-1}$ based on the experimental data.

Figure 4(a) shows current-voltage characteristics of the ZnO p-n homojunction. Clear rectifying behavior can be observed with and without UV illumination. The turn-on voltage is at ~ 3 V. The possible formation of the graded p-n junction due to the impurity diffusion during nanowire growth and the formation of the metal/semiconductor nanowire contact are the reasons for the small rectification ratio of the p-n homojunction. Photocurrent (PC) measurements were carried out using a homebuilt system. The PC system consists of an Oriel Xe arc lamp as the UV source. The light from the lamp passes through an Oriel 0.25 m monochromator, which produces a specific wavelength light at its output port. After chopping, the light is then cast on the device. The generated PC signal is fed to a lock-in amplifier from where the data are collected. Figure 4(b) shows PC spectra of

the homojunction device operated in the photovoltaic mode and also under different reverse biases. The device shows response as a result of the photocarriers generated by the absorption of light in the space-charge region. The response extends from 280 nm and steadily increases up to 380 nm (3.26 eV), which corresponds to the effective band gap of ZnO. The magnitude of photocurrent increases with the increase of applied reverse bias (-2 , -4 , and -6 V) due to enhanced carrier collection. There is a small peak at 570 nm (2.17 eV) in the spectra due to the presence of deep levels in ZnO.

In summary, ZnO p-n homojunctions based on Sb-doped p-type nanowire arrays and n-type thin films were grown by the combination of CVD and MBE. The ZnO thin film/nanowire p-n junction was proved by EBIC profiling, I-V measurement, and field-effect measurement. Evident photoresponse was observed in the UV region of the PC spectra. This study not only proved that Sb doping can lead to p-type ZnO nanowires, but also demonstrated an ultraviolet homojunction photodetector device based on p-type nanowire array and n-type thin film.

Guoping Wang and Sheng Chu contributed equally to this work. This research was partly supported by National Science Foundation (Grant No. ECCS-0900978).

¹E. O. Kane, *Phys. Rev. B* **18**, 6849 (1978).

²C. Klingshirn, *Phys. Status Solidi B* **244**, 3027 (2007).

³D. C. Look, *Mater. Sci. Eng., B* **80**, 383 (2001).

⁴S. Chu, J. H. Lim, L. J. Mandalapu, Z. Yang, L. Li, and J. L. Liu, *Appl. Phys. Lett.* **92**, 152103 (2008).

⁵H. Cao, Y. G. Zhao, H. C. Ong, S. T. Ho, J. Y. Dai, J. Y. Wu, and R. P. Chang, *Appl. Phys. Lett.* **73**, 3656 (1998).

⁶S. F. Yu, C. Yuan, S. P. Lau, W. I. Park, and G. Yi, *Appl. Phys. Lett.* **84**, 3241 (2004).

⁷S. Chu, M. Olmedo, Z. Yang, J. Y. Kong, and J. L. Liu, *Appl. Phys. Lett.* **93**, 181106 (2008).

⁸L. J. Mandalapu, F. X. Xiu, Z. Yang, D. T. Zhao, and J. L. Liu, *Appl. Phys. Lett.* **88**, 112108 (2006).

⁹L. J. Mandalapu, Z. Yang, F. X. Xiu, D. T. Zhao, and J. L. Liu, *Appl. Phys. Lett.* **88**, 092103 (2006).

¹⁰L. J. Mandalapu, F. X. Xiu, Z. Yang, and J. L. Liu, *Solid-State Electron.* **51**, 1014 (2007).

¹¹C. H. Chen, S. J. Chang, S. P. Chang, M. J. Li, I. C. Chen, T. J. Hsueh, and C. L. Hsu, *Appl. Phys. Lett.* **95**, 223101 (2009).

¹²O. Lupan, T. Pauporte, and B. Viana, *Adv. Mater.* **22**, 3298 (2010).

¹³X. M. Zhang, M. Y. Lu, Y. Zhang, L. J. Chen, and Z. L. Wang, *Adv. Mater.* **21**, 2767 (2009).

¹⁴C. G. Van de Walle, *Phys. Rev. Lett.* **85**, 1012 (2000).

¹⁵D. K. Hwang, H. S. Kim, J. H. Lim, J. Y. Oh, J. H. Yang, S. J. Park, K. K. Kim, D. C. Look, and Y. S. Park, *Appl. Phys. Lett.* **86**, 151917 (2005).

¹⁶K. K. Kim, H. S. Kim, D. K. Hwang, J. H. Lim, and S. J. Park, *Appl. Phys. Lett.* **83**, 63 (2003).

¹⁷T. S. Jeong, M. S. Han, C. J. Youn, and Y. S. Park, *J. Appl. Phys.* **96**, 175 (2004).

¹⁸F. X. Xiu, Z. Yang, L. J. Mandalapu, D. T. Zhao, and J. L. Liu, *Appl. Phys. Lett.* **87**, 152101 (2005).

¹⁹L. E. Greene, M. Law, D. H. Tan, M. Montano, J. Goldberger, G. Somorjai, and P. D. Yang, *Nano Lett.* **5**, 1231 (2005).

²⁰L. Chernyak, C. Schwarz, E. S. Flitsiyan, S. Chu, J. L. Liu, and K. Gartsman, *Appl. Phys. Lett.* **92**, 102106 (2008).

²¹S. Hoffmann, J. Bauer, C. Ronning, Th. Stelzner, J. Michler, C. Ballif, V. Sivakov, and S. H. Christiansen, *Nano Lett.* **9**, 1341 (2009).

²²S. Limpijumnong, S. B. Zhang, S. H. Wei, and C. H. Park, *Phys. Rev. Lett.* **92**, 155504 (2004).

²³R. Martel, T. Schmidt, H. R. Shea, T. Hertel, and Ph. Avouris, *Appl. Phys. Lett.* **73**, 2447 (1998).